Koc. J. Sci. Eng., 7(1): (2024) 42-51 https://doi.org/10.34088/kojose.1295098

Kocaeli University

Kocaeli Journal of Science and Engineering

http://dergipark.org.tr/kojose

Topology Optimization of Structural Drive-Train Component of an Electric-Driven Vehicle for Additive Manufacturing

Ahmet Erkan KILIÇ [1], Atilla SAVAŞ [2,*], Yavuz YÜCESOY [3]

[1] *Department of Mechanical Engineering, Piri Reis University, İstanbul, 34940, Turkey,* ***ORCID:*** *0000-0002-5782-6132*
[2] *Department of Mechanical Engineering, Piri Reis University, İstanbul, 34940, Turkey,* ***ORCID:*** *0000-0001-6900-3259*
[3] *Department of Mechanical Engineering, Piri Reis University, İstanbul, 34940, Turkey,* ***ORCID:*** *0000-0002-9556-7872*

Article Info

Research paper

Received : *May 10, 2023*
Accepted : *October 10, 2023*

Keywords

Additive Manufacturing
Finite Element Analysis
Manufacturing
Topology Optimization

Abstract

Additive Manufacturing (AM) is an emerging technology and an important alternative to conventional manufacturing methods as it enables the production of lighter parts that are potentially more durable. In this context, the design for additive manufacturing (DFAM) has been drawing a considerable amount of attention mainly in the aerospace, and automotive industries as well as in academia. On the other hand, the ability of additive manufacturing to manufacture complex topology is often the outcome of topology optimization, which makes topology optimization a good design tool for additive manufacturing. The main objective of the present work is to redesign a structural component of the drivetrain of the Shell Eco-Marathon vehicle, with the use of Altair Inspire™, an industrial generative design tool, by application of Topology Optimization for Additive Manufacturing aiming mass reduction and does not cover the print process.

1. Introduction

Additive Manufacturing (AM) is a state-of-the-art method that brings a transformative approach to industrial production enabling the creation of lighter, potentially stronger parts. The design of lightweight structures via AM methods has been attracting a considerable amount of consideration in academia and industries for a wide range of applications.

However, the capability to additively manufacture complicated parts is the result of topology optimization (TO), which makes TO an excellent instrument for AM.
The additive behavior is opposed to material removal processes such as milling, cutting, drilling, etc. which start with a bulk of material and step by step remove the material to reach the final part" [1].

According to the American Society for Testing and Materials [1], AM is *"the process of joining materials to make objects from 3D model data, usually layer upon layer, as opposed to subtractive manufacturing methodologies."*

Different materials can be used in different AM technologies. AM machines and 3D printers can be easily used in the production of polymers, metals, ceramic materials, paper, wood, cork, foam, and rubber, including in layered manufacturing.

As AM technology develops further and the costs of 3D printed parts begin to decrease, AM and 3D printing will become the more widely used method. To make full use of this technology, ways to take advantage of one of its various advantages, the Topology Optimization technology, will be sought.[2].

When used together with machining methods, AM provides more flexibility to the designer, and the cost differences in producing complex parts are eliminated.

Thanks to the studies in Metallic AM in recent years, functional products have started to be used instead of prototypes. Industrialists seem very willing to take advantage of this. It does not seem logical to produce the existing design with the AM method. It is necessary to redesign the part to be produced and take advantage of TO.

* Corresponding Author: asavas@pirireis.edu.tr

The targets in production have led to the use of different optimization methods. Three types of optimization methods have been developed for production via the AM method:

Size optimization -

Shape optimization -

Topology optimization -

TO is an essential element in making the most of the features AM enables for design.

TO can roughly be separated into the management of two different types of domains: continuum and distinct structures. Distinct structures often refer to large constructions like bridges, cranes, and other truss structures, while continuum structures often refer to smaller, single-piece parts and components [3]

The most widely used software density-based TO method is also called SIMP (Solid Isotropic Material with Penalization method).

Plosher and Panesar made studies about design for Additive Manufacturing [4]. These authors stated that although AM design methods are widely used today, the numerical methods used for many engineering problems are still not widely used in the market.

Liu et al. He gave information about how to use the TO methods used before 3D printers and AM methods.[5].

Langelaar's work discusses the key features of an additive manufacturing process and a filter that can be used in density-based TO procedures.[6].

In the study carried out by Atzeni and Salmi, it is evaluated that the parts produced by the additive manufacturing method compete with the parts produced by machining and this causes production increases.[7].

Christiansen et al. stated that the optimized part uses only 20% of the material compared to machining.[8]. They utilized the DSC method (Deformable Simplicial Complex method). TO has proven to be a good technique for designing bone replacements [9]. Mezzadri et al. formulated the creation of support structures for AM as a TO problem [10]. Chu et al. utilized a SIMP-based method to cope with the TO of multi-material structures with cascading interfaces [11]. Zheng et al. suggested an orderly method to design robust multi-material parts under gap loading uncertainty [12].

The work presented by Xu et al. can be seen as a useful step towards a more realistic and comprehensive framework for integrating stress-constrained stiffness design and the topological design of geometrically nonlinear structures [13].

Liu et al. aimed to create a reliable topological design by considering local material uncertainties in their work [14]. Li et al. presented a meshless method that was developed for the TO problem of structures under multiple loading conditions [15]. Bi et al. presented a new method that can effectively address protruding features in the bi-directional evolutionary structural optimization framework [16].

A kind of derivative respirator was developed based on FDM (Fused Deposition Modeling) by Aydın et al. [17]. Çelebi and Tosun utilized the FDM method to produce a router and managed to save 60 percent of the volume and mass [18].

Shell Eco-Marathon is a worldwide competition for student teams which they participate with their vehicles. The competition aims to encourage students to design and manufacture their vehicles through high-tech and energy-efficient solutions.

The objective of Shell Eco-Marathon is to build the most energy-efficient car. Therefore, the weight of the car components is of critical importance.

In this present study, the electric motor bracket of an all-electric Shell Eco marathon vehicle has been redesigned for additive manufacturing with the use of Altair Inspire™, an industrial generative design tool, by application of Topology Optimization for Additive Manufacturing aiming mass reduction. The scope of the study is limited to the redesigning and does not cover the print process.

The results of finite element analysis that have been performed on the redesigned part show that the redesigned part is capable of withstanding applied loads while the part is in operation.

Moreover, a significant mass reduction is achieved with the redesigned model in comparison to the original model.

The method used by Christiansen et al. made only 20 percent of the material be used for production [8]. In our case, 89 percent scrap reduction is achieved which is a good result compared to the mentioned case.

2. Materials and Methods

2.1. Topology Optimization and Structural Modeling of The Part

The part considered for this work is an electric motor holder. For TO, Altair Inspire™ software was used.

The electric motor holder of an electric vehicle to be used in this study is shown in Figure 1.

The current, voltage, and similar values of the electric motor are given in Table 1. The torque and speed relations for the motor are depicted in Figure 2.

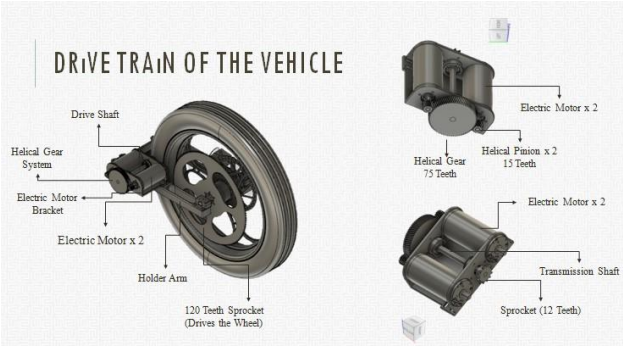

Figure 1. Electric motor, gearbox, transmission shaft, and electric motor holder [19]

Table 1. Technical data and specifications of the Direct Current Motor

Data	Value
Nominal Voltage	24 VDC
Nominal Current	10.8 A
Maximum Speed	9500 RPM (No Load)
Nominal Speed	5680 RPM
Maximum Efficiency	94%
Maximum Torque	8920 mN-m (Stall Torque)

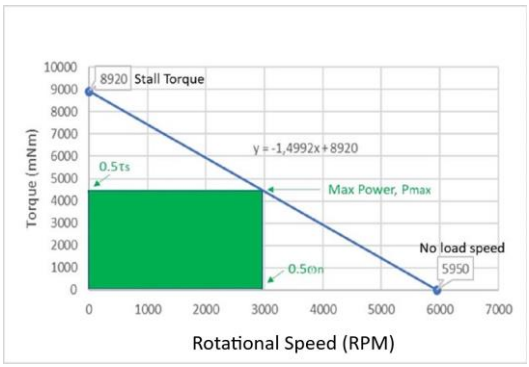

Figure 2. D.C. Motor Torque Speed Curve

2.2. Torque–Power Calculations

The Maximum Power is obtained at the mid-speed of the motor, 2975 RPM. The Torque at that speed is 4460 mNm.

Power is defined as:

$$P = T\omega \text{ [20]} \quad (1)$$

where P represents power in watts, T represents torque in N.m and ω represents the rotational speed in rad/s.

2.3. Transmission Specifications and Gear Force Analysis

The schematic diagram of the Gear Train (Transmission) is given in Figure 3.

Two pinions one for each Electric Motor drive the Gear. Data for the pinions and the gear are as follows:

Pinions: 15 teeth (Z_1) helical gears with 20° normal pressure angle (Φ_n), 1 mm normal module (m_n), and a helix angle of 20° (Ψ)

Gear: 75 teeth (Z_2) helical gear with 20° normal pressure angle (Φ_n), 1 mm normal module (m_n), and a helix angle of 20° (Ψ)

The formula given below can be utilized to compute the transverse pressure angle of a helical gear:

$$\tan\Phi_n = \tan\Phi\cos\Psi \quad (2)$$

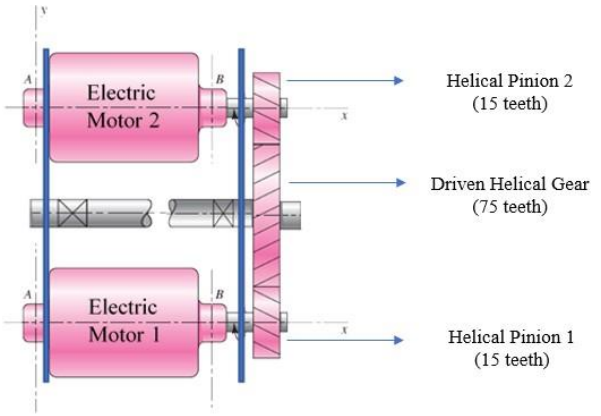

Figure 3. D.C. Motors and Gear Train [19]

The module for a helical gear is defined as:

$$m = m_n/\cos\Psi \quad (3)$$

The pitch diameter for helical gears is defined as:

$$d_1 = mZ_1 \quad \text{[20]} \quad (4)$$

Pitch line velocity for a helical gear is defined as:

$$V = \pi d_1 n_1/60 \quad [20] \tag{5}$$

As depicted in Figure 4, at the pitch point C of the pinion, the force Fr acts in the y-axis, Fa acts in the x-axis, and Ft acts in the z-axis.

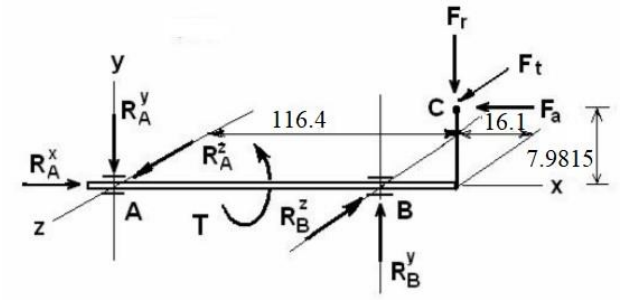

Figure 4. Diagram indicating the forces in action at the pitch point C of the pinion. [19]

Figure 5 illustrates the applied forces and the directions in which they act on Pinion-1 and the Driven Helical Gear, while Figure 6 presents the applied forces and their respective directions for Pinion-2 and the Driven Helical Gear.

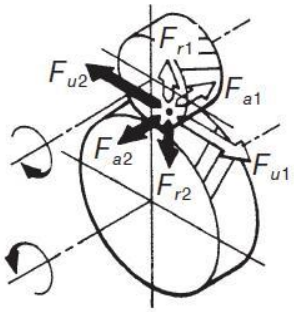

Figure 5. Pinion 1 and Driven Gear. [19]

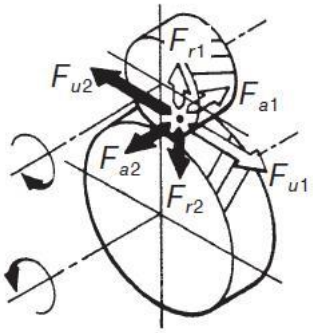

Figure 6. The second pinion and the gear that is being driven by it. [19]

Now both the torque and rotational speed values of the shaft that is being driven by the gear can be computed.
The gear ratio is defined as:

$$Gear\ Ratio = Z_2/Z_1 \quad [20] \tag{6}$$

Therefore, the gear ratio is 5
So, at P_{max}, the speed at which the shaft that is being driven will be;
n_2 = 595 *RPM*.
Also;

$$Gear\ Ratio = \text{Torque out}/\text{Torque in} \quad [20] \tag{7}$$

Torque out / Torque in = 5;
Then; Torque out = 4.46 x 5 = 22.3 *Nm* = 22300 *mNm*.

2.4. The Bracket Design

In the first stage, it is necessary to mark the places of the motor holder part is to be optimized and the places that will not be optimized. It will be possible to save material in the areas marked as areas to be optimized. The places that will not be optimized are usually close to the bearings and there will be no opportunity to save material in these places. [21].

The spaces that are going to be optimized are depicted in brown color and the spaces that are not going to be optimized are shown in grey color. The fixed support is also shown in the figure below (Figure 7.).

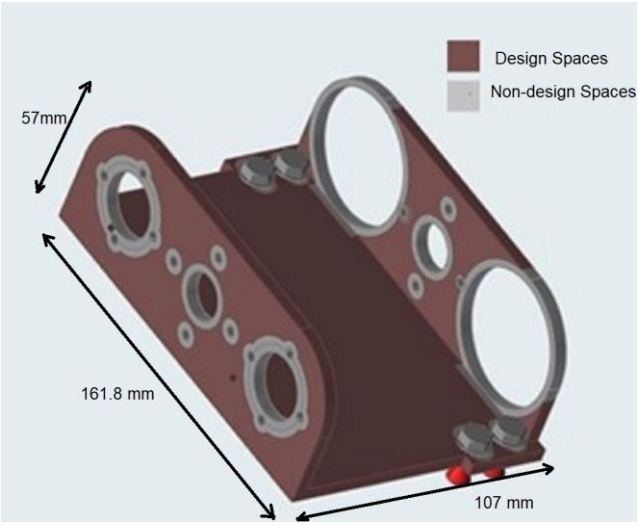

Figure 7. Design and Non-Design Spaces of the Bracket, fixed supports

Material selection is also an important parameter. The basic material of the Electric Motor holder is 7075 Al alloy. However, 7075 Al alloy is an underused material for AM technology. Considering this fact, AlSi10Mg, the closest material to this one and is widely used in AM technology, has been chosen.

Mechanical and thermal expansion information for AlSi10Mg material [5], [22] tabulated in Table 2. These

values are considered in the Altair Inspire™ commercial code. The structural analysis is performed via these tabulated values.

Table 2. Material data for *AlSi10Mg*

Material	**E** (*GPa*)	**Poisson's Ratio**	**Density** (*g/cm³*)	**Yield Stress** (*MPa*)	**Tensile Strength** (*MPa*)	**CTE** (*μm/m °K*)
AlSi10Mg	70	0.33	2.67	215	335	20

2.4.1. Shape Control Application

There are two different ways to control geometry in Inspire™. These are called symmetry and drawing directions. The simultaneous utilization of them is not appropriate and only one is allowed. [23]

Apart from the drawing direction tools in Inspire™, only the protrusion tool is suitable with AM method. The protrusion tool aims to create self-supporting parts. In processes such as casting and extrusion, draw direction tools other than the protrusion tool can be used. [23]

In this study, both the protrusion tool and the symmetry tool were used. Figures 8. a and 8. b show the multiple complex loading states, constraints, protrusion tool, and symmetry tool applied to the part under study.

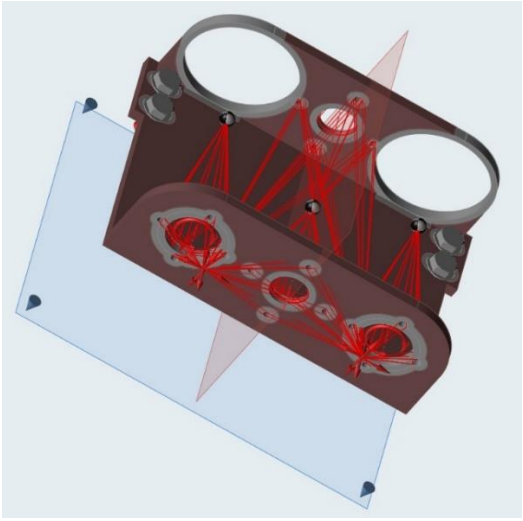

Figure 8.a Various loads, and limitations applied to the original electric motor bracket model.

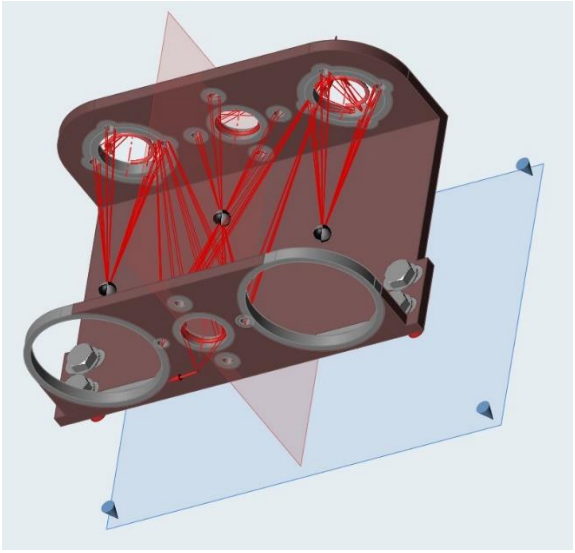

Figure 8.b An alternative perspective of various loads and limitations applied to the original electric motor bracket model.

2.5. Topology Optimization Run

In the next step, the TO process will be run using the previously defined material properties, constraints, and geometry properties.

In TO processes, material saving is only applied in the brown areas shown in Figure 7. The aim is to remove as much material as possible from the part without reducing the strength of the material. In TO operation, the Altair Inspire™ allows the installer to maximize strength or minimize mass.

Once these goals are set, the design constraints on the part need to be applied. If the designer chooses the goal of the study to be strength maximization, a mass target for TO has to be set and entered into the Inspire program. [7].

If the designer sets a wall thickness limit, the TO cycle time can be extended. The Inspire software has the ability to determine the minimum wall thickness by taking into account the average size of the elements in the part [4].

2.6. Redesign of the Part with Inspire PolyNURBS

The PolyNURBS application is part of the Inspire programme. With this application, the irregularly shaped part obtained as a result of the TO application is given a smooth geometry. The part obtained with this method is shown in Figure 9.

Figure 9. Redesigned Model with the Use of PolyNURBS

3. Results and Discussion

3.1. Calculations

For the topology optimization to be performed, we will be based on the Pmax condition of the D.C. motor in order to be more on the conservative side for the final design.

Per this, taking equation 1 and electric motor technical data given in Figure 4 into consideration, P_{max} as well as torque and rotational speed at P_{max} were calculated as below.

Table 3. Pmax, torque and rotational speed at Pmax

P_{max}	1.39 kW
T (at P_{max})	4.46 Nm
Rotational Speed	2975 RPM

Based on the calculations provided in Table-3 and given the

Ψ=20^o (helical angle)

Φ_n= 20^o (normal pressure angle)

m_n= 1 mm (normal module)

Z_1 = 15 (number of teeth on the pinion)

Z_2 = 75 (number of teeth on the helical gear)

results provided in Table-2 were calculated.

Table 4. calculations relating to Gearbox for Pmax condition

ϕ (transverse pressure angle for helical gear)	21.17°
m (module for a helical gear)	1.0642 mm
d1 (pitch diameter of the pinion)	15.963 mm
V (pitch line velocity for helical gear)	2.487 m/sec
n2 (rotational speed of the driven shaft)	595 RPM
Torque Out (at Pmax)	22.3 Nm

Acting forces are calculated as shown below:

F_t = 1000 W / V = 1000 x 1.39 / 2.487 = 558.906 N

$F_r = F_t \tan \Phi$ = 558.906 x tan 21.17^o = 216.449 N

$F_a = F_t \tan \Psi$ = 558.906 x tan 20^o = 203.425 N

$F_n = F_t / \cos \Phi_n \cos \Psi$ = 558.906 / (cos 20^o x cos 20^o) = 635.963 N

3.2. Mass of the Redesigned Model

When comparing the mass of the initial design and the newly created design of the original bracket. under examination, the mass of the designed model as determined by the Altair Inspire™ analysis is 0.24 kg per bracket. While the manufacturing mass of the initial component is 0.35 kg; Based on topology optimization of the aforementioned bracket with additive manufacturing designed using Altair Inspire™, it was determined that the redesign reduced the mass of the part by 31% (0.11 kg).

3.3 The process of reducing waste through the use of the modified model.

Waste minimization emerges as another important advantage of the designed model and its fabrication using additive manufacturing according to the original design and original production technique. It has been calculated that 2.8 kg of AA7075 billet will be required in the production of the original design with known manufacturing techniques. Considering that the final production mass is 0.3 kg, unfortunately, 89% (2.8 kg) of the material is spent as scrap in the production of brackets made in this context.

In addition, as a result of the realization of the designed new model with the suggested additive manufacturing method, the benefit of discarding 2.8 kg of material in the classical method is also obtained. Considering that the amount of scrap in the part designed using the AM technique is 0.11 kg, when 2.5 kg of waste obtained in the classical method of the motor bracket is added, 2.6 kg of material will be saved between both methods and in favor of production with AM technology. According to Christiansen et al., only 20% of the material was utilized for manufacture [8]. Comparatively speaking, our case's 89 percent scrap reduction is a good outcome. The only purpose of this study is to use the additive manufacturing method as the boundary condition for the optimization study.

3.4 Finite Element Analysis of PolyNURBS Results

The Altair Inspire™ program was used for a Finite Element Analysis, which is the performance parameters of the model bracket designed with the help of AM technology, such as yield safety factor, von Misses stresses, and rupture

safety factor.

The yield stress comprehensive safety factor analysis results obtained from the aforementioned program are given in Figure 10 and Figure 11. The ultimate safety factor results obtained from the same program are given in Figure 12 and Figure 13. Besides, Figure 14 and Figure 15 show the von Misses Stress Analysis results.

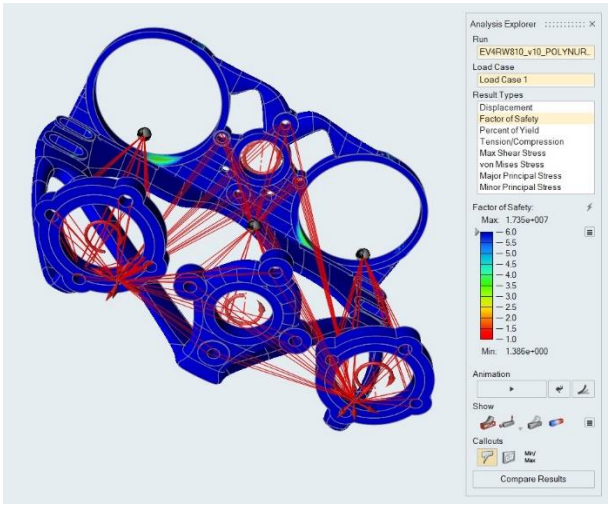

Figure 10. Analysis Results for Factor of Safety for Yielding

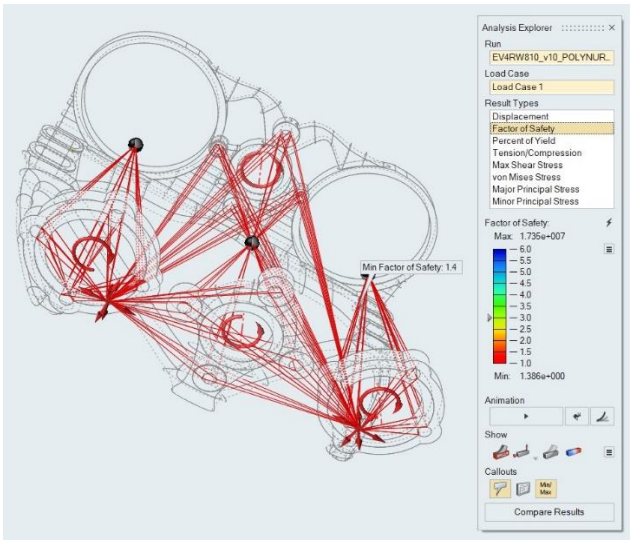

Figure 11. Analysis Results for Factor of Safety for Yielding Showing Minimum FOS Location

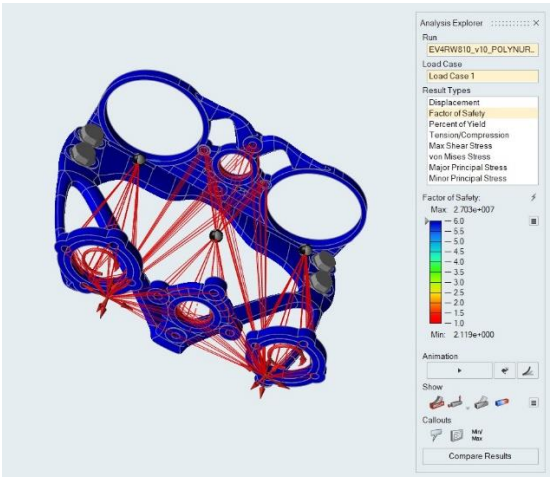

Figure 12. Analysis Results for Ultimate Factor of Safety

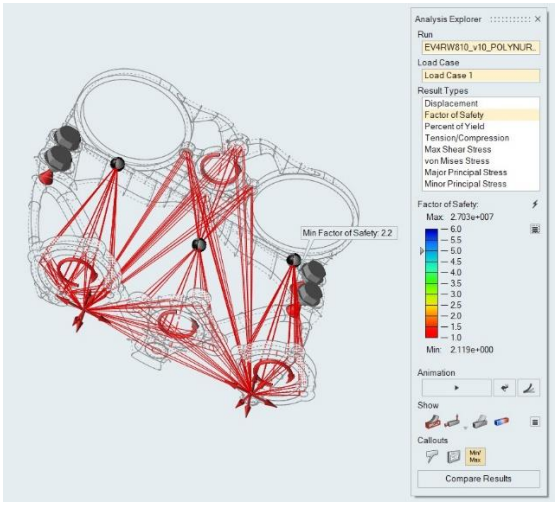

Figure 13. Analysis Results for Ultimate Factor of Safety showing the location where the factor of safety for the ultimate minimum value is achieved.

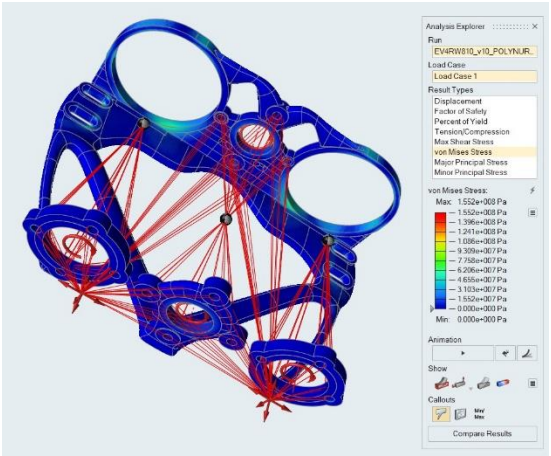

Figure 14. The findings of the examination of v. Mises stress.

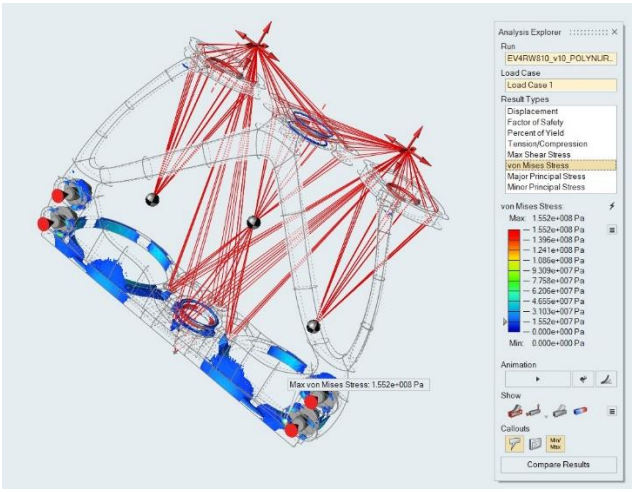

Figure 15. The results of the analysis of von Mises stress indicating the location where the highest stress is present.

3.5 Interpretation of FEA Results and Discussion

When looking at Figures 10 and 11, the minimum safety factor for yielding is determined to be 1.4 and is in the safe zone when the design criterion of 1.25 is taken into account. This result proves that the maximum load on the support remains within the elastic range of the stress-strain curve as intended under the operating conditions of the system in question.

Examination of the analysis results for the maximum factor of safety yielded the results shown in Figures 12 and 14 and showed that the factor in question is ~2.1. This value is considered safe as the maximum safety factor exceeds the aviation standard of 1.5.

In the final phase of the investigation, a stress analysis was performed according to the von Misses criterion and the stress distributions obtained are shown in Figures 14 and 15. As a result of the analysis, a maximum stress of 155.2 MPa was determined in the analyzed part. The yield stress of the material (AlSi10Mg) from which the part is made is 215 MPa. Therefore, the part in the redesigned geometry will be in the elastic range even at Pmax, where the force transmission elements are not exposed at all.

As a result of all these analyses of the redesigned model using the AM method, it has been shown that the part functions safely even under the worst working conditions without exceeding the elasticity limits.

4. Conclusions

In the summary of this study, the tested bracket to be manufactured from 7075 Al alloy was modeled using Altair Inspire™, without changing its original dimensions, as a basis for production by AM method.

The newly designed part was proposed to be manufactured from AlSi10Mg alloy, the most commonly used Al alloy for AM applications. The FEA of the newly molded part in the area of the maximum load of the DC motors resulted in a minimum safety factor of 1.25, which corresponds to the design requirements of 1.4.

The mass of the part which was re-shaped using topology optimization, was diminished by 37%, obtaining 229 grams, concerning the original mass of 364 grams while 89% scrap reduction was achieved compared to the original design via later machining methods.

When examining the results of this study, it was found that the newly designed model, when realized through additive manufacturing, met the strength criteria and would function without structural degradation. In addition, the structural mass was reduced and a significant gain in waste minimization was achieved.

Declaration of Ethical Standards

The authors of this article declare that the materials and methods used in this study do not require ethical committee permission and/or legal-special permission.

Conflict of Interest

The authors declare that they have no known competing financial interests or personal relationships that could have appeared to influence the work reported in this paper.

Abbreviations and Symbols

AM	Additive Manufacturing
CTE	Coefficient of Thermal Expansion
FDM	Fused Deposition Modeling
FEA	Finite Element Analysis
SIMP	Solid Isotropic Material with Penalization Method
TO	Topology Optimization
d_1	Pitch diameter of the pinion
F_a	Force in the x-direction
F_r	Force in the y-direction
F_t	Force in the z-direction
F_u	Force in the tangential axis
m	Module
m_n	Normal module
n_1	Rotational speed of helical gear 1 (RPM)
n_2	Rotational speed of helical gear 2 (RPM)
P	Power (W)
T	Torque (Nm)
V	Pitch line velocity
Z_1	15 teeth helical gear
Z_2	75 teeth helical gear

Φ Pressure angle
Φ_n Normal pressure angle
ω Rotational speed (rad/s)
Ψ Helix angle

References

[1] ASTM INTERNATIONAL, "ASTM F2792-12a," *Rapid Manufacturing Association*, pp. 1–3, 2013, doi: 10.1520/F2792-12A.2.

[2] Clausen, A., 2015. Topology Optimization for Additive Manufacturing,". doi: 10.1017/CBO9781107415324.004.

[3] Gornet T., 2017 "History of Additive Manufacturing,". doi: 10.4018/978-1-5225-2289-8.ch001.

[4] Plocher J. and Panesar A., 2019, Review on design and structural optimization in additive manufacturing: Towards next-generation lightweight structures, Mater Des, **183**, p. 108164, doi: 10.1016/j.matdes.2019.108164.

[5] Liu J. *et al.*, 2018, Current and future trends in topology optimization for additive manufacturing, Structural and Multidisciplinary Optimization, **57**, no. 6, pp. 2457–2483, 2018, doi: 10.1007/s00158-018-1994-3.

[6] Langelaar M., 2017, An additive manufacturing filter for topology optimization of print-ready designs, Structural and Multidisciplinary Optimization, **55**, no. 3, pp. 871–883, 2017, doi: 10.1007/s00158-016-1522-2.

[7] Atzeni E. and Salmi A., 2012, Economics of additive manufacturing for end-usable metal parts, International Journal of Advanced Manufacturing Technology, **62**, no. 9–12, pp. 1147–1155, 2012, doi: 10.1007/s00170-011-3878-1.

[8] Christiansen A.N., Bærentzen J.A., Nobel-Jørgensen M., Aage N., and Sigmund O., 2015. Combined shape and topology optimization of 3D structures, *Computers* and Graphics (Pergamon), **46**, pp. 25–35, 2015, doi: 10.1016/j.cag.2014.09.021.

[9] J. Park J., A. Sutradhar A., Shah J. J., and Paulino G. H., 2018. Design of complex bone internal structure using topology optimization with perimeter control, Comput Biol Med, **94**, pp. 74–84, Mar. 2018, doi: 10.1016/j.compbiomed.2018.01.001.

[10] Mezzadri F., Bouriakov V., and Qian X., 2018. Topology optimization of self-supporting support structures for additive manufacturing, Addit Manuf, **21**, pp. 666–682, May 2018, doi: 10.1016/j.addma.2018.04.016.

[11] Chu S. , Xiao M., Gao L., Li H., Zhang J., and Zhang X., 2019. Topology optimization of multi-material structures with graded interfaces, Computer Methods Appl Mech Eng, **346**, pp. 1096–1117, Apr. 2019, doi 10.1016/j.cma.2018.09.040.

[12] Zheng Y, Da D., Li H., Xiao M., and Gao L., 2020. Robust topology optimization for multi-material structures under interval uncertainty, Appl Math Model, **78**, pp. 627–647, Feb. 2020, doi: 10.1016/j.apm.2019.10.019.

[13] Xu B., Han Y., and Zhao L., 2019. Bi-directional evolutionary topology optimization of geometrically nonlinear continuum structures with stress constraints," Appl Math Model, **80**, pp. 771–791, Apr. 2020, doi: 10.1016/j.apm.2019.12.009.

[14] Liu B., Jiang C., Li G., and Huang X., 2020. Topology optimization of structures considering local material uncertainties in additive manufacturing, Computer Methods Appl Mech Eng, **360**, Mar. 2020, doi: 10.1016/j.cma.2019.112786.

[15] Li J., Guan Y., Wang G., Wang G., Zhang H., and Lin J., 2020. A meshless method for topology optimization of structures under multiple load cases, Structures, **25**, pp. 173–179, Jun. 2020, doi: 10.1016/j.istruc.2020.03.005.

[16] Bi M., Tran P., and Xie Y.M., 2020. Topology optimization of 3D continuum structures under geometric self-supporting constraint, Addit Manuf, **36**, Dec. 2020, doi 10.1016/j.addma.2020.101422.

[17] Aydın L. *et al.*, 2021. Development of Personal Protective Respirator Based on Additive Manufacturing Technologies in Fighting Against Pandemic, Kocaeli Journal of Science and Engineering, **4**, no. 1, pp. 24–38, May 2021, doi: 10.34088/kojose.833205.

[18] Çelebi A. and Tosun A., 2021. Application and Comparison Of Topology Optimization For Additive Manufacturing And Machining Methods, Int. J. of 3D Printing Tech. Dig. Ind, **5**, no. 3, pp. 676–691, 2021, doi: 10.46519/ij3dptdi.

[19] Sakarya University Advanced Technologies Application Center (SAITEM), www.saitem.org.

[20] Budynas R.G., Nisbett J.K., 2011. Shigley's Mechanical Engineering Design, 9th edition, Macgraw Hill, New York.

[21] Diegel O., Nordin A., and Motte D., 2019. A Practical Guide to Design for Additive Manufacturing. 2019. doi: 10.1007/978-981-13-8281-9.

[22] Verbart A., 2015. Topology Optimization with Stress Constraints. 2015. doi: 10.4233/uuid: ee24b186-5db6-4c57-aa50-3b736110ff2a.

[23] Altair Inspire: Generate Structurally Efficient Concepts Quickly and Easily. https://altair.com/inspire